Science Advances

AAAS

advances.sciencemag.org/cgi/content/full/3/7/e1700939/DC1

Supplementary Materials for

Catalysis beyond frontier molecular orbitals: Selectivity in partial hydrogenation of multi-unsaturated hydrocarbons on metal catalysts

Wei Liu, Yingda Jiang, Karl-Heinz Dostert, Casey P. O'Brien, Wiebke Riedel, Aditya Savara, Swetlana Schauermann, Alexandre Tkatchenko

Published 26 July 2017, *Sci. Adv.* **3**, e1700939 (2017)
DOI: 10.1126/sciadv.1700939

This PDF file includes:

Supplementary Text

The 1-butene molecule on Pt(111)

It has been widely accepted that the FMO theory is a very useful tool for understanding reaction mechanisms of molecules and the interactions of small molecules on metal surfaces, e.g., 1-butene on the Pt(111) surface. As shown in fig. S1, the HOMO of 1-butene, which is spatially located on the C=C double bond, is significantly perturbed upon interaction with the catalyst. According to the FMO theory, 1-butene is activated preferentially at the C=C, which in excellent agreemment with experimental findings that the hydrogenation reactions occur exclusively at the C=C bond of 1-butene.

Hydrogenation reaction barrier at low and high coverage for isophorone on Pd(111)

A more direct link to the experimental observables – the reaction rates – was obtained by computing the activation barriers for isophorone partial hydrogenation over the Pd(111) surface. We determined the structure of the transition state using the linear/quadratic synchronous transit method (*19*). At low coverage, we found that the energy barriers are 0.61 and 1.08 eV, respectively, for the first and second hydrogenation step at the C=C bond, being significantly smaller than those when hydrogen atoms attack the C=O bond (0.99 and 1.40 eV, respectively). Similarly, the desorption energy of the C=C bond hydrogenation product (1.14 eV) is also smaller than that of the C=O hydrogenation product (1.57 eV). This further supports that hydrogenation of the C=C bond is highly preferred over the C=O bond on Pd(111). The whole reaction process is shown in fig. S2. At high coverage, we found that the energy barriers are 0.62 and 0.56 eV, respectively, for the first and second hydrogenation step at the C=O bond, being significantly smaller than those when hydrogen atoms attack the C=C bond (3.46 and 0.84 eV, respectively).

Computed adsorption structure and binding energy for isophorone/Pd(111) in a (4×4) unit cell

Our PBE+vdW^{surf} calculations reproduce well the adsorption structure obtained from experiments. The preferable structure for isophorone on the clean Pd(111) surface is shown in Fig. 2C in the main text. The O−Pd and C−Pd distances for the C=O and C=C double bonds are in the range of 2.18 to 2.29 Å, close to typical covalent bond lengths. In contrast, carbon atoms in the three methyl groups attached to the ring, which are highly affected by the vdW forces, are lifted above the surface by 2.87 to 5.05 Å. The C=C bond in the adsorbed isophorone was found to be elongated by 0.1 Å as compared to the isolated molecule (from 1.35 to 1.45 Å), suggesting a change of the effective bond order of the C=C bond. The carbonyl bond was found to be elongated to a lesser extent (from 1.23 to 1.29 Å). Note that the correct adsorption structure for isophorone on Pd(111) can only be obtained when vdW interactions are correctly

accounted for in our calculations. More specifically, the standard PBE functional, with no vdW interactions, predicted that the C=C bond in isophorone tilts upon adsorption. This structure hinders the adsorption and activation of the C=C bond, and would predict an incorrect selectivity to the unsaturated alcohol. The vdW interactions also dramatically enhance the binding energy from 0.58 (PBE) to 1.79 eV (PBE+vdW^{surf}), due to the relatively short adsorption distance between the adsorbate and the substrate. Besides the most perferable structure shown in Fig. 2C, in our calculations, we have also carefully explored the potential-energy surface for isophorone on the Pd(111) surface in a (4×4) unit cell. We relaxed a single isophorone molecule at eight adsorption sites of the metal substrate, which are denoted as top30°, bri30°, fcc30°, hcp30°, top0°, bri0°, fcc0°, and hcp0° (fig. S3). Note that the oxygen was taken as reference in the molecule, since all stable configurations correspond to this atom, which forms covalent bonds with Pd atoms at the Pd(111) surface. After full relaxation, two optimized binding configurations were obtained by using the PBE+vdW^{surf} method.

Isophorone on the surfaces of Pd(111), Pt(111), Rh(111), Ir(111), Cu(111), Ag(111), and Au(111)

To demonstrate that the proposed "orbital broadening mechanism" is a general phenomenon that exists for a variety of molecules and metallic surfaces message, we carried out extensive calculations for isophorone on other six transition-metal surfaces, including Cu(111), Ag(111), Au(111), Pt(111), Rh(111), and Ir(111). Similar to benzene, the nature of bonding for isophorone on these substrates can be classified into two types: strongly bound systems (on Cu, Ag, and Au) and weakly bound systems (on Pd, Rh, and Ir). By analysis the MODOS plots in fig. S4, it is interesting to note that the HOMO-1 orbital localized at the C=C bond is strongly broadened upon interaction with Pt(111), Rh(111), and Ir(111) surfaces. This agrees with experimental observations that reactive metals such as Pd, Pt, Rh and Ru are typically observed to be more prone to hydrogenate the C=C double bond, similarly to the case of isophorone/Pd reported here. In contrast, high selectivities in C=O bond hydrogenation in unsaturated carbonyl compounds are typically observed over noble metals such as Ag and Au. Generally, the molecules are weakly interacting with these noble metals and perform supposedly more like their gas-phase counterparts. Weaker interacting systems – such as noble metals – are expected to show much lesser extent or no broadening effect on the inner molecular orbitals, which can be clearly seen in fig. S4B for isophorone on Cu(111), Ag(111), and Au(111) surfaces. Consequently, the selectivity toward hydrogenation of the C=C bond is expected to decrease on these metals, while the relative amount of C=O hydrogenation events should increase, resulting in a total increase of the selectivity toward hydrogenation of the carbonyl group.

Acrolein on the surfaces of Pd(111), Pt(111), Rh(111), Ir(111), Cu(111), Ag(111), and Au(111)

To further generalize our finding, we continued to study the smallest α,β-unsaturated aldehyde acrolein over seven transition-metal surfaces (fig. S5). Similar to isophorone, our calculations clearly

demonstrated that the inner orbital of acrolein is also significantly broadened in strongly bound systems. As exemplified by the most extensively studied acrolein/Pd(111) system, a consensus conclusion from many experiments is that essentially only the C=C bond of acrolein can be hydrogenated over the Pd(111) surface forming propanal (*6*, *12*, *18*). This observation can be well explained in the scope of our model. As shown in Fig. 4, the HOMO-1 spatially located around the C=C double bond is significantly broadened upon interaction with Pd(111), which is accompanied by a large amount of charge transfer from the inner orbital to the substrate. Similar phenomenon can also be clearly seen in other strongly bound systems, such as acrolein on Pt(111), Rh(111), and Ir(111), leading to the activation and preferential hydrogenation of the C=C double bond. These theoretical predictions based on the extent of broadening of inner molecular orbitals are in a good qualitative agreement with the large body of experimental observations. Therefore, we conclude that the proposed orbital broadening mechanism is a general phenomenon that exists for a variety of molecules and metallic surfaces, and can be utilized to explain many other practically-relevant chemoselective reactions.

Coadsorption of hydrogen atom on Pd(111)

Notably, we did not coadsorb hydrogen atoms in our models. This is mainly because our experimental IRAS data clearly showed that the C=C and C=O bonds are lying flat at low coverage, no matter whether the hydrogen atoms are coadsorbed or not on the Pd(111) surface. Besides that, as soon as the IRAS vibration appears, the C=C and C=O vibrations are at the same frequency as on the clean surface, indicating that the binding to the Pd is not so different. Therefore, it is reasonable to use the pure Pd(111) surface, without including the pre-adsorbed hydrogen atoms in our models. To check the validity of our model, we have further considered coadsorbed hydrogen atoms in our models. We found that the existence of hydrogen atoms in the system does not significantly modify the adsorption structure and electronic properties of the adsorbed isophorone molecule. The adsorption structures with and without including the hydrogen atom is shown in fig. S6.

Isophorone on Pd(111) at high coverage

To deeply understand the selective hydrogenation reaction, we studied the isophorone on Pd(111) at high coverage. The Pd(111) surface was modeled by periodic (3×2) unit cell. As shown in fig. S7A, compared to the parallel structure between molecule and substrate at low coverage, the isophorone tilts and the C=C bond keeps away from the metal surface. That orientation in turn of molecule leads to completely different interaction with the surface, including adsorption energetics and electronic structure. The adsorption energy is decreased to -0.83 eV at high coverage, comparing to which is -1.66 eV at low coverage. By analysis the MODOS plot in fig. S7B, it is interesting to note that the HOMO orbital localized at the C=O bond is strongly broadened upon interaction with Pd(111) surface.

Comparison between the experimental and calculated vibrational spectra for isophorone on the Pd(111) surface

Finally, we would demonstrate that in addition to adsorption structure, our calculations can also reproduce well the vibration spectra obtained from experiments. Fig. 3A displays the vibrational spectrum (upper curve) obtained after the exposure of about $1.5 \cdot 10^{14}$ isophorone molecules$\cdot$cm^{-2} (~0.1 monolayer as referenced to the number of surface Pd atoms) on Pd(111) at 120 K. For comparison, the calculated vibrational spectrum of the gas phase molecule is also plotted. Three main spectral regions can be distinguished, which are characteristic of C−H stretching vibrations (2800−3200 cm^{-1}), C=C and C=O stretching (1550−1850 cm^{-1}), as well as for C−H deformation vibrations (< 1500 cm^{-1}). While the exact assignment of the stretching and deformation vibrations of C−H bonds is rather complex and lies beyond the scope of this work, the vibrational features corresponding to the C=C and C=O bonds are indicative of the adsorption geometry of these molecules on the substrate. As evident from the comparison of the calculated isophorone gas phase spectrum and the spectrum obtained on Pd surface, the features corresponding to C=C and C=O vibrations are missing for the surface-adsorbed species. This is a consequence of the metal surface selection rule, resulting in a strong attenuation of the vibrational modes parallel to the surface.

To scrutinize the feasibility of the calculated structures, the anharmonic IR spectra were computed for isophorone on Pd(111) using *ab initio* molecular dynamics simulations at 130 K (Fig. 3A, lowest curve). The simulations were run for up to 73 picoseconds, and the calculated spectra on Pd(111) agree very well with the experimentally measured IR spectra showing a vanishing of C=O and C=C stretching modes as expected for a flat-lying isophorone. For the high frequency region of C−H stretching vibrations (2200−2900 cm^{-1}), there is good qualitative agreement between the calculated and the measured spectra for isophorone.

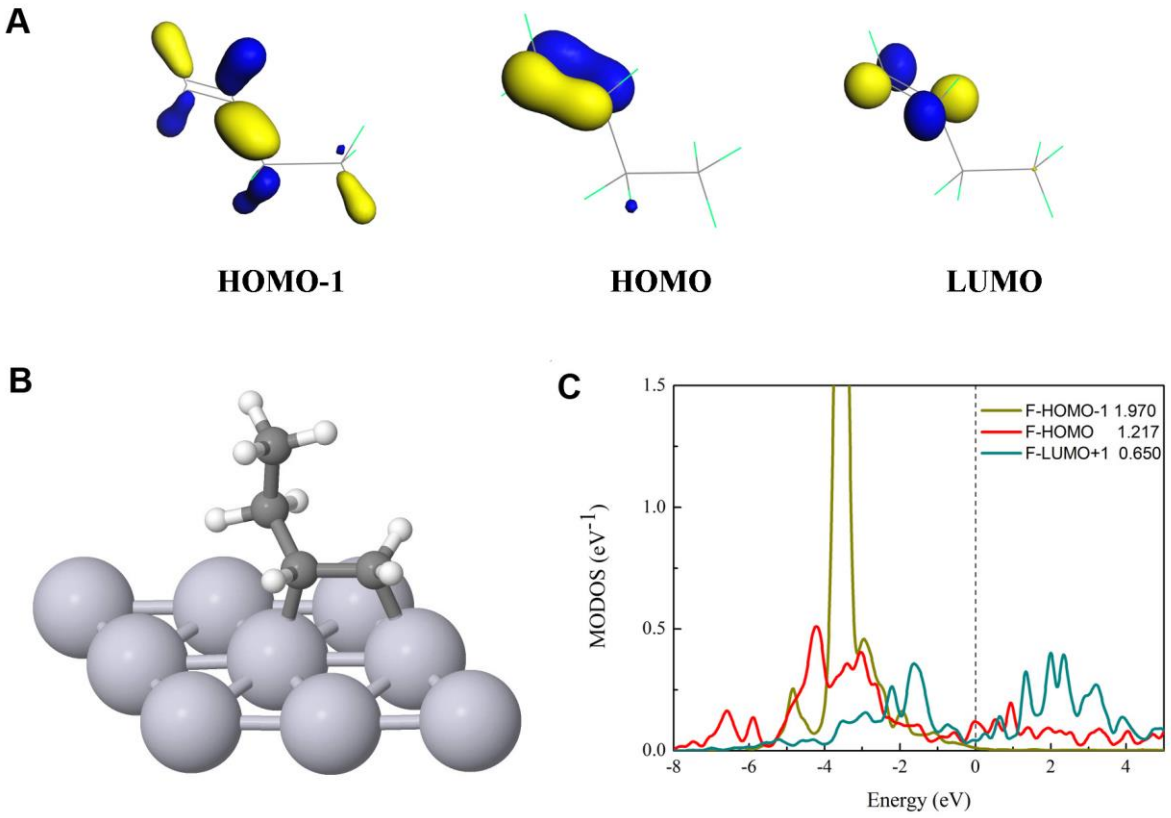

fig. S1. Structure and electronic properties of 1-butene. (**A**) The HOMO-1, HOMO, and LUMO molecular orbitals for the isolated 1-butene molecule. (**B**) The relaxed structure for 1-butene on the Pt(111) surface. (**C**) MODOS projected on the free 1-butene (C_4H_8) HOMO-1, HOMO, and LUMO orbitals for 1-butene over the Pt(111) surface. The zero of energy corresponds to the Fermi level.

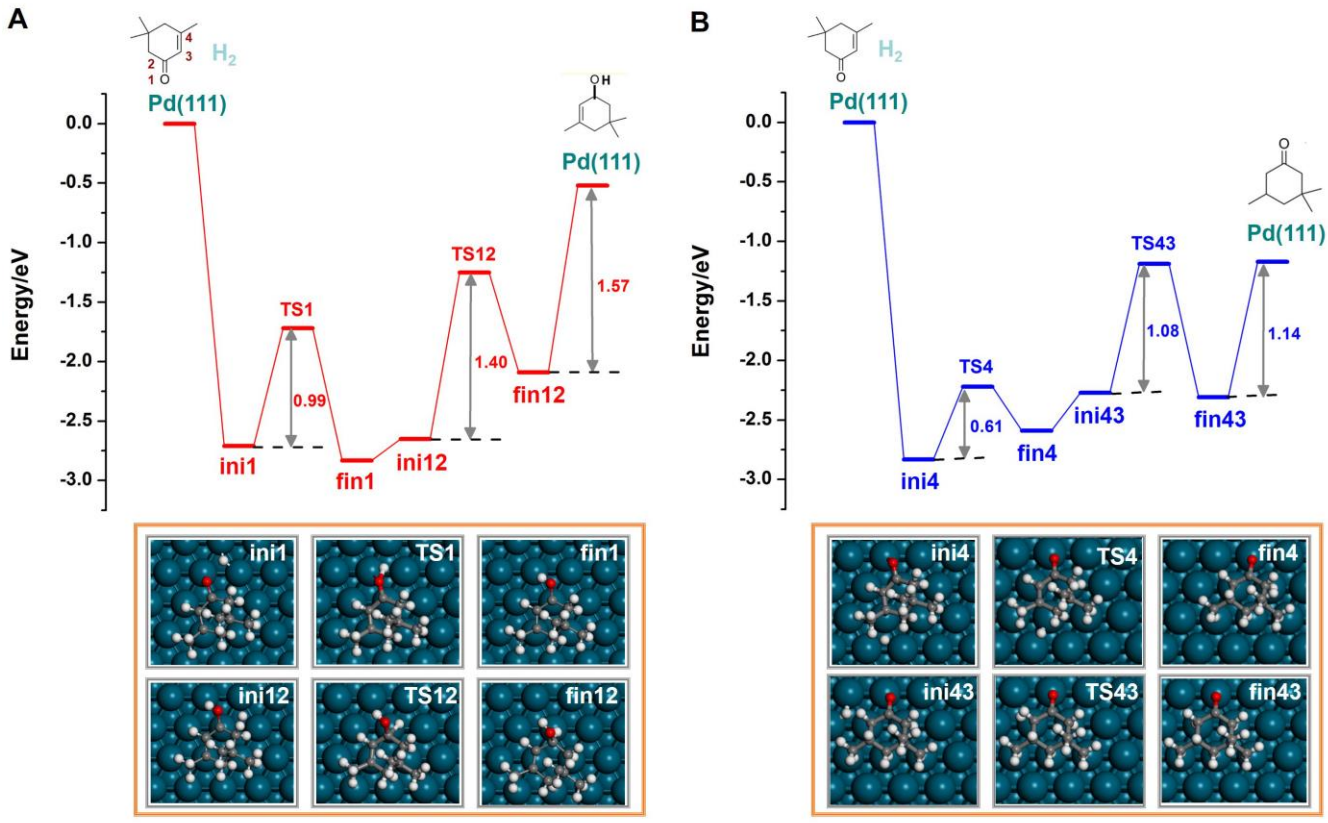

fig. S2. Hydrogenation pathways of isophorone on Pd(111). Calculated energy profiles of isophorone hydrogenation to (**A**) isophorol (**B**) trimethylcyclohexanone at Pd(111) and the structures of the corresponding transition states (TS1, TS12 and TS4, TS43) and the initial, final states (ini1, fin1, ini12, fin12 and ini4, fin4, ini43, fin43). For clarity, the oxygen and carbon atoms involved in hydrogenation have been numbered in the isophorone molecule. Pd atoms are in glaucous, C in grey, H in white, and O in red.

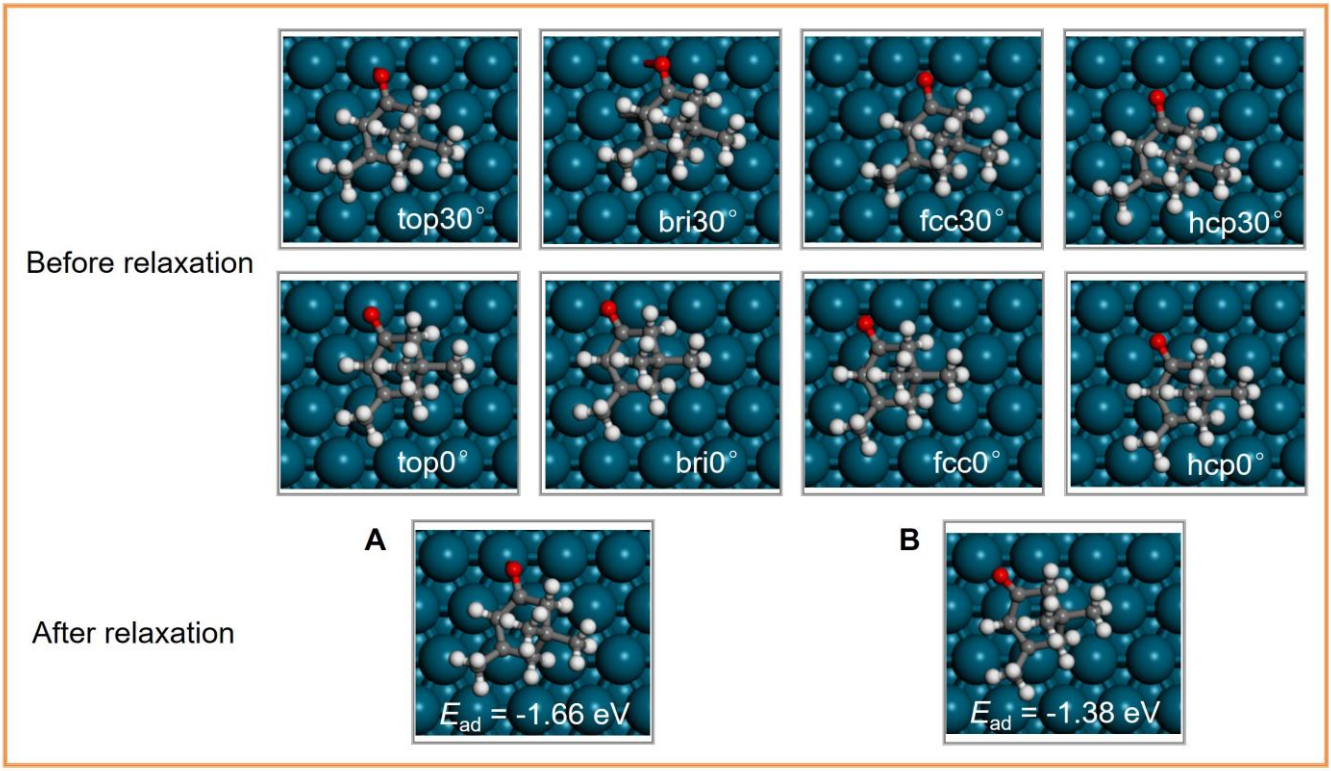

fig. S3. Adsorption structures of isophorone on Pd(111). The oxygen atom was taken as reference in the molecule; at each site, the carbon ring has two orientations, *i.e.* 0° and 30°, referring to the angles of the C−C bond being rotated with respect to the neighboring metal−metal bond. After relaxation, top30°, bri30°, fcc30°, hcp30°, top0° and hcp0° convert to the adsorption structure shown in (**A**). Similarly, bri0° and fcc0° convert to the structure shown in (**B**).

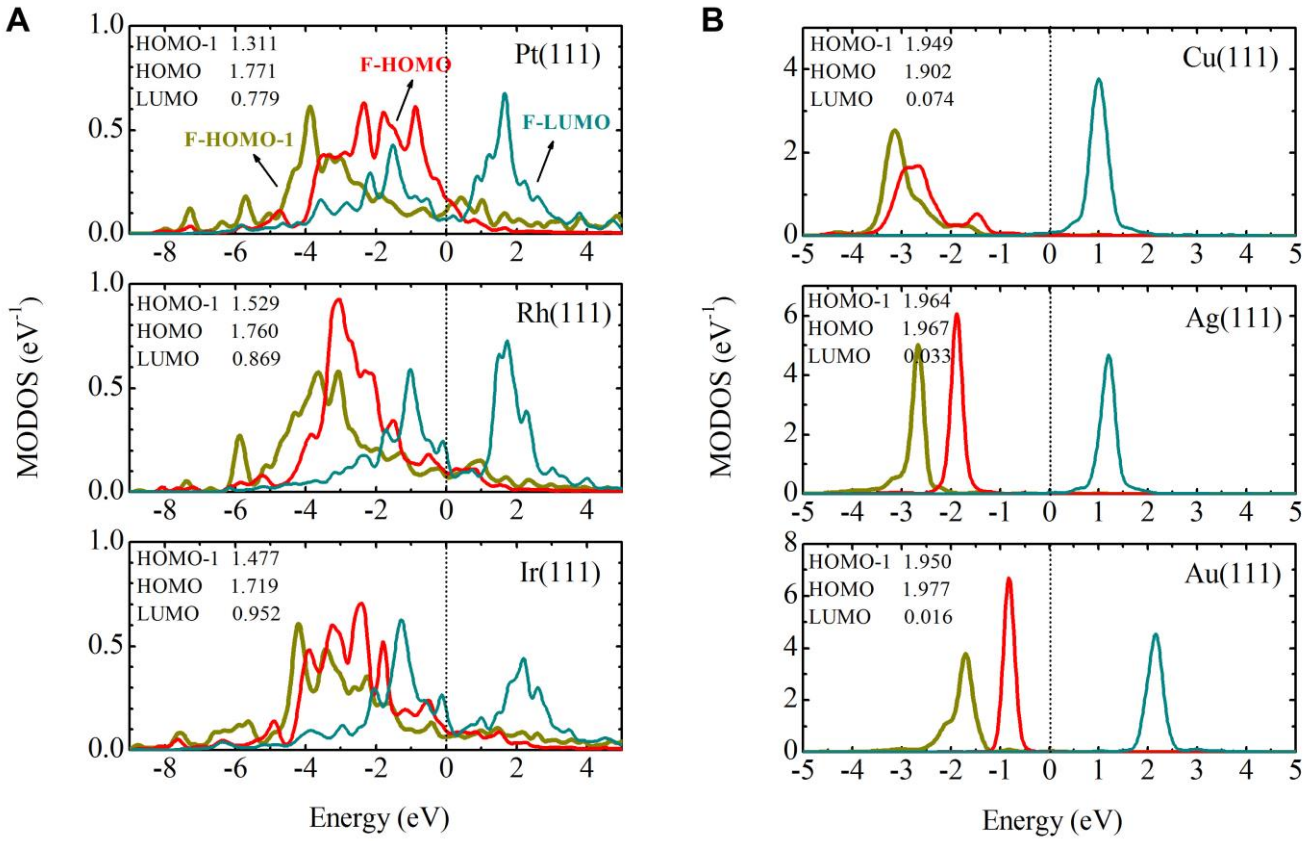

fig. S4. MODOS of isophorone on metal surfaces. MODOS projected on the free isophorone HOMO-1, HOMO, and LUMO orbitals for (**A**) strongly bound systems and for (**B**) weakly bound systems. The zero of energy corresponds to the Fermi level. The computed projected occupation of selected molecular orbitals near the Fermi level is also shown in this plot.

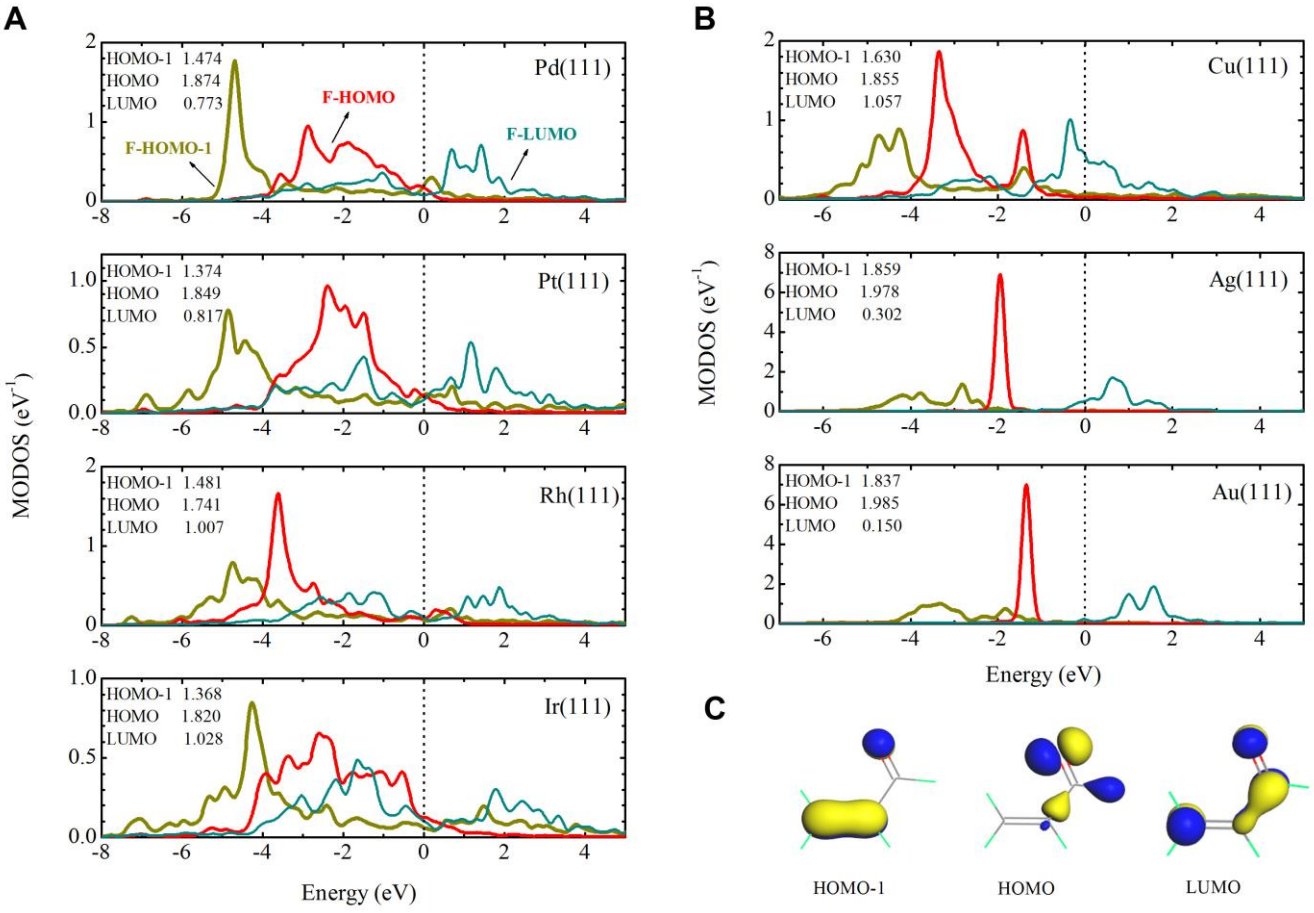

fig. S5. MODOS of acrolein on metal surfaces. The MODOS projected on the free acrolein (C_3H_4O) HOMO-1, HOMO, and LUMO orbitals for (**A**) strongly bound systems and for (**B**) weakly bound systems. The zero of energy corresponds to the Fermi level. The computed projected occupation of selected molecular orbitals near the Fermi level is also shown in this plot. (**C**) The HOMO-1, HOMO, and LUMO molecular orbitals for the isolated acrolein molecule.

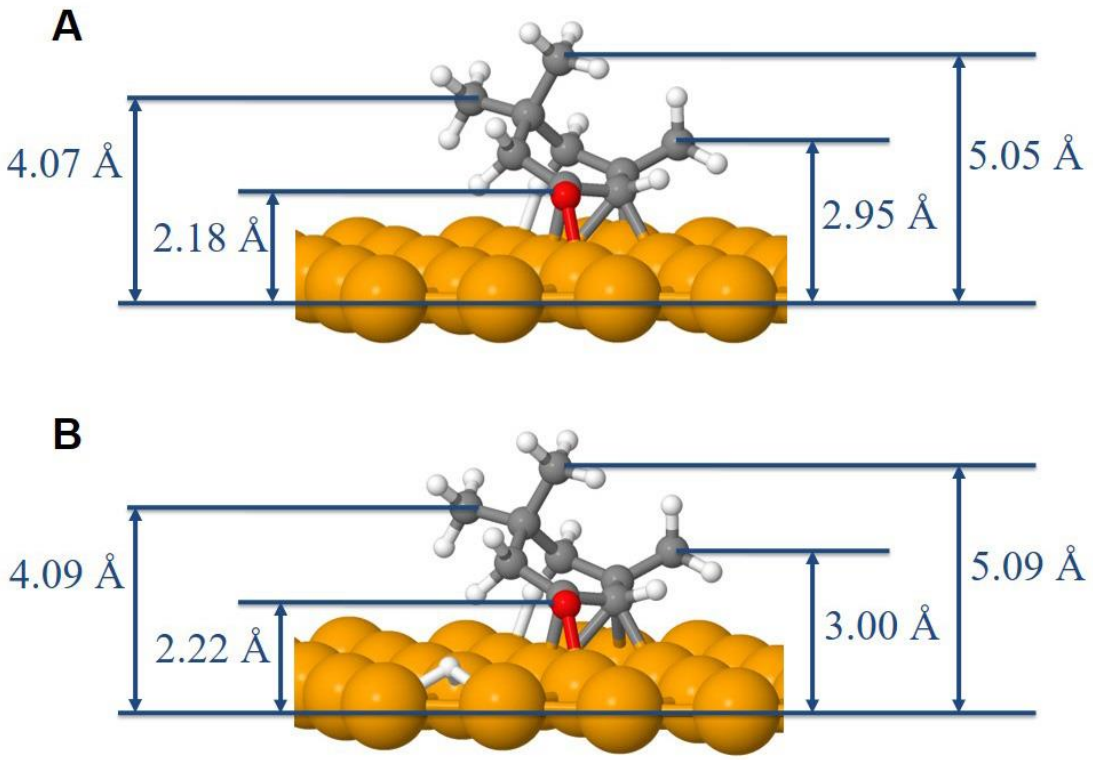

fig. S6. Coadsorption structure of isophorone on Pd(111). Adsorption structures for isophorone adsorbed on the Pd(111) surface (**A**) without and (**B**) with co-existence of a hydrogen atom.

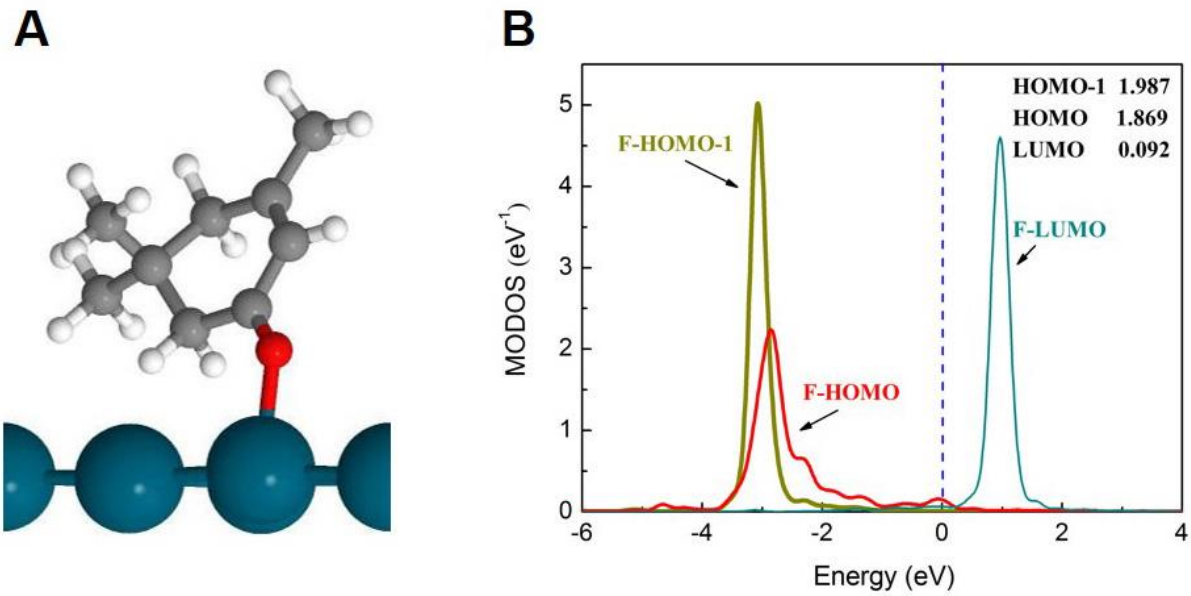

fig. S7. Isophorone on Pd(111) at high coverage. (**A**) Adsorption structure for isophorone adsorbed on the Pd(111) surface at high coverage. (**B**) MODOS projected on the free isophorone ($C_9H_{14}O$) HOMO-1, HOMO, and LUMO orbitals for Pd(111). The zero of energy corresponds to the Fermi level. The projected occupation of selected molecular orbitals near the Fermi level is also shown in this plot.